Route to observable Fulde-Ferrell-Larkin-Ovchinnikov phases in three-dimensional spin-orbit-coupled degenerate Fermi gases

Zhen Zheng, Ming Gong, Xubo Zou, Chuanwei Zhang, and Guangcan Guo

Phys. Rev. A **87**, 031602 — Published 22 March 2013

DOI: 10.1103/PhysRevA.87.031602

New Route to Observable Fulde-Ferrell-Larkin-Ovchinnikov Phases in 3D Spin-Orbit Coupled Degenerate Fermi Gases

Zhen Zheng[1], Ming Gong[2],* Xubo Zou[1],† Chuanwei Zhang[2],‡ and Guangcan Guo[1]
[1]*Key Laboratory of Quantum Information, University of Science and Technology of China, Hefei, Anhui, 230026, People's Republic of China*
[2]*Department of Physics, the University of Texas at Dallas, Richardson, TX, 75080 USA*

The Fulde-Ferrell-Larkin-Ovchinnikov (FFLO) phase was first predicted in 2D superconductors about 50 years ago, but so far unambiguous experimental evidences are still lacked. The recently experimentally realized spin-imbalanced Fermi gases may potentially unveil this elusive state, but require very stringent experimental conditions. In this Letter, we show that FFLO phases may be observed even in a 3D degenerate Fermi gas with spin-orbit coupling and in-plane Zeeman field. The FFLO phase is driven by the interplay between asymmetry of Fermi surface and superfluid order, instead of the interplay between magnetic and superconducting order in solid materials. The predicted FFLO phase exists in a giant parameter region, possesses a stable long-range superfluid order due to the 3D geometry, and can be observed with experimentally already achieved temperature ($T \sim 0.05E_F$), thus opens a new fascinating avenue for exploring FFLO physics.

PACS numbers: 67.85.Lm, 03.75.Ss, 74.20.Fg

The Fulde-Ferrell-Larkin-Ovchinnikov (FFLO) phase, characterized by Cooper pairs with finite total momentum and spatially modulated order parameters, was predicted to exist in certain region of 2D superconductors in high Zeeman fields [1–3]. This fascinating state arises from the interplay between magnetic and superconducting order, and now is a central concept for understanding many exotic phenomena in different physics branches [4–12]. Despite tremendous experimental and theoretical efforts in the past five decades, there is still no unambiguous experimental evidence for FFLO states [11]. The experimental difficulty may arise from several different aspects, such as the depairing of Cooper pairs due to orbital or Pauli effects in strong magnetic fields and unavoidable disorder effects in solid state materials.

The recent experimental realization of spin-imbalanced Fermi gases [13–17] provides a new excellent platform for exploring FFLO physics. In Fermi gases, the effective Zeeman field is generated through the population imbalance between two spins, therefore the orbital effects (e.g., vortices induced by the magnetic field) are absent even in 3D. The Fermi gases are also free of disorder and all experimental parameters are highly controllable. These advantages have sparked tremendous recent interest in exploring FFLO physics in spin-imbalanced Fermi gases [18–28]. However, the FFLO phase only exists in a narrow parameter regime in 3D due to the Pauli depairing effect[18, 22, 23]. Furthermore, the free energy difference between the FFLO state and the BCS superfluid is extremely small. As a result, only the transition from the BCS superfluid to the normal gas [13–15] has been observed in 3D spin-imbalanced Fermi gases. Current experimental and theoretical efforts on the FFLO state have focused on low dimensions system [29–33], where quantum and thermal fluctuations may become crucial and the physics is much more complicated [34–36].

In this Letter we show that a large and stable parameter region for FFLO states can be realized even in a 3D degenerate Fermi gas by including two experimentally already developed [37–39] elements: spin-orbit (SO) coupling and an in-plane Zeeman field. Recently the BCS-BEC crossover physics of SO coupled Fermi gases with perpendicular Zeeman fields has been intensively investigated with the goal of realizing topological superfluids [40–43] and the associated Majorana fermions [44–46]. However, regular BCS superfluids, instead of FFLO states, are energetically preferred for perpendicular Zeeman field. We show that this issue can be resolved by using an in-plane Zeeman field, which, together with the SO coupling, yields an asymmetric Fermi surface so that the FFLO state can emerge naturally. We emphasize that here the FFLO phase is driven by the asymmetry of the Fermi surface, instead of population imbalance. More importantly, we find that the energy difference between the FFLO ground state and the possible BCS superfluid excited state is dramatically increased (to $\sim 0.04E_F$ per particle), therefore the FFLO state is experimentally more accessible with the realistic temperature in 3D ($T \sim 0.05E_F$). Because of the 3D geometry, the quantum and thermal fluctuations are strongly suppressed[34–36] therefore greatly simplifies the FFLO physics. Finally, we argue that our system has no direct solid state analogy and the new route represents a more efficient way to create and observe FFLO phases.

Thermodynamical potential: Consider a 3D degenerate Fermi gas in the presence of a Rashba type of SO coupling and an in-plane Zeeman field. The partition function of the system can be expressed as $Z = \mathrm{Tr}e^{-\beta(H-\mu N)} = \int \mathcal{D}\psi e^{-S}$, with the action $S = \int \psi^\dagger(\partial_\tau + H_0)\psi + g\psi^\dagger_\uparrow\psi^\dagger_\downarrow\psi_\downarrow\psi_\uparrow$. Here $\int = \int_0^\beta d\tau d^3\mathbf{r}$, $\psi^\dagger = (\psi^\dagger_\uparrow, \psi^\dagger_\downarrow)$, $H_0 = \frac{\mathbf{p}^2}{2m} - \mu - h\sigma_x + \alpha(p_x\sigma_y - p_y\sigma_x)$, m is the mass of the

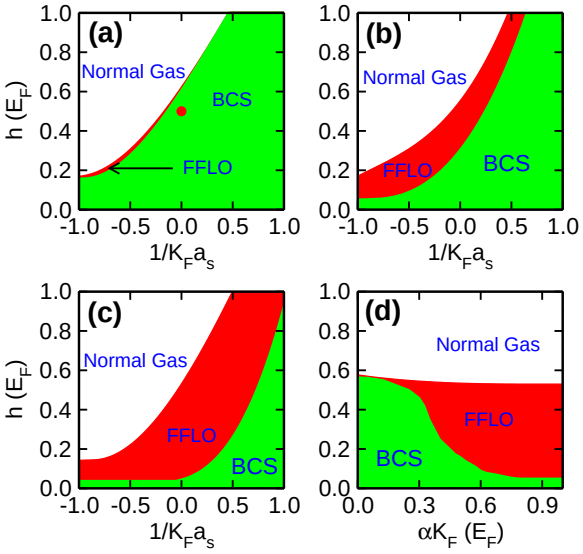

FIG. 1: (Color online). BCS-BEC crossover phase diagrams in the presence of SO coupling and in-plane Zeeman field. (a) Without SO coupling. The circle symbol represents the data from the quantum Monte Carlo calculation [52]. (b) and (c) With $\alpha K_F = 0.5E_F$ and $\alpha K_F = 1.0E_F$. (d) In the unitary regime.

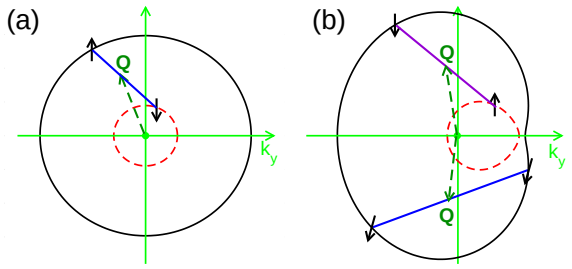

FIG. 2: (Color online). Illustration of the physical mechanism of the FFLO state in the presence of an in-plane Zeeman field and SO coupling. Solid and dashed contours are two Fermi surfaces. The solid arrows are the pseudospins. The solid line connecting two pseudospins represents the Cooper pair with total momentum $\mathbf{Q}$ (dashed arrow). (a) Without SO coupling, the Fermi surfaces are two concentric spheres. (b) With SO coupling, the Fermi surfaces are anisotropic along the k_y axis due to the Rashba SO coupling and the x-axis Zeeman field.

atom, μ is the chemical potential, g is the s-wave interaction strength, α is the Rashba SO coupling strength, and h is the in-plane (same as the SO coupling) Zeeman field. In experiments, the SO coupling and the in-plane Zeeman field can be realized using the tripod scheme where three Raman lasers couple three hyperfine ground states with a common excited state [47–49]. Note that an in-plane Zeeman field is generated naturally in the tripod scheme [47–49], while a perpendicular Zeeman field requires additional lasers [50] (thus more difficult in experiments).

In the FFLO state the Cooper pairs have finite total momentum, *i.e.*, $\Delta(\mathbf{r}) = \langle\psi_\downarrow\psi_\uparrow\rangle = \Delta e^{i\mathbf{Q}\cdot\mathbf{r}}$, where $\mathbf{Q}$ is the FFLO vector. We adopt a spatial uniform order parameter Δ in our calculation through a transformation of the field $\psi \to \psi e^{i\mathbf{Q}\cdot\mathbf{r}/2}$, yielding a new Hamiltonian $e^{i\mathbf{Q}\cdot\mathbf{r}/2}H_0(\mathbf{p})e^{i\mathbf{Q}\cdot\mathbf{r}/2} = H_0(\mathbf{p}+\mathbf{Q}/2) = \bar{H}_0$, hence

$$S = \int \psi^\dagger(\partial_\tau + \bar{H}_0)\psi - |\Delta|^2/g + \Delta\psi_\uparrow^\dagger\psi_\downarrow^\dagger + \Delta^\dagger\psi_\downarrow\psi_\uparrow \quad (1)$$

in the new field basis. Integrating out the Fermi field, we obtain $Z = \int \mathcal{D}\Delta \exp(-S_{\rm eff})$, with the effective action

$$\frac{S_{\rm eff}}{\beta} = -\frac{|\Delta|^2}{g} - \sum_{\lambda,\mathbf{k},i\omega_n} \frac{\ln\beta(i\omega_n - E_\lambda)}{2\beta} + \sum_{\mathbf{k},\sigma} \frac{\xi_{\frac{\mathbf{Q}}{2}-\mathbf{k},\sigma}}{2}, \quad (2)$$

where $\xi_{\frac{\mathbf{Q}}{2}-\mathbf{k},\sigma} = (\frac{\mathbf{Q}}{2}-\mathbf{k})^2/2m - \mu$, E_λ ($\lambda = 1, 2, 3, 4$) are the eigenstates of the effective Hamiltonian (under the basis $(\psi_{\mathbf{Q}/2+\mathbf{p},\uparrow}, \psi_{\mathbf{Q}/2+\mathbf{p},\downarrow}, \psi^\dagger_{\mathbf{Q}/2-\mathbf{p},\downarrow}, -\psi^\dagger_{\mathbf{Q}/2-\mathbf{p},\uparrow})^T$)

$$H_{\rm eff}(\mathbf{k},\mathbf{Q}) = \begin{pmatrix} H_0(\frac{\mathbf{Q}}{2}+\mathbf{k}) & \Delta \\ \Delta^\dagger & -\sigma_y H_0^*(\frac{\mathbf{Q}}{2}-\mathbf{k})\sigma_y \end{pmatrix}. \quad (3)$$

In Eq. (2) the bare interaction strength g should be regularized in terms of the s-wave scattering length a_s [41, 43], $\frac{1}{4\pi\hbar a_s} = \frac{1}{g} + \sum_{\mathbf{k}} \frac{1}{2\epsilon_{\mathbf{k}}}$, where $\epsilon_{\mathbf{k}} = \frac{k^2}{2m}$.

The ground state phase diagram of the system (i.e., Δ, μ, $\mathbf{Q}$) is determined by the saddle point of the thermodynamical potential $\frac{\partial\Omega}{\partial\Delta} = 0$ and $\frac{\partial\Omega}{\partial\mathbf{Q}} = 0$, as well as the atom number conservation[51], $n = \sum_{\sigma=\uparrow,\downarrow} n_\sigma = -\frac{\partial\Omega}{\partial\mu}$, where $\Omega = S_{\rm eff}/\beta$. The energy unit is chosen as the Fermi energy E_F for an non-interacting gas without SO coupling and Zeeman field. The length unit is K_F^{-1}. We restrict to $T = 0$ throughout this work. Generally the vector $\mathbf{Q}$ has three different components, and the total five unknown parameters put a great burden for numerically solving the above equations self-consistently because the landscape of Ω is an extremely complex function of these parameters whose global minimum (instead of a local minimum) is hard to find. For the x-axis Zeeman field and the Rashba-type SO coupling the deformation of the Fermi surface is along the y-axis, therefore the FFLO vector is expected to be along the y axis, *i.e.*, $\mathbf{Q} = (0, Q, 0)$. We have numerically confirmed that there is no large FFLO region when $\mathbf{Q}$ is along the x and z directions. There are three possible phases in this system: BCS superfluid ($\Delta \neq 0$, $Q = 0$) (we still use BCS for convenience although we really consider the BCS-BEC crossover physics), FFLO ($\Delta \neq 0$, $Q \neq 0$), and normal gas ($\Delta = 0$ and $Q = 0$). In the FFLO phase, we also calculate the energy difference between the FFLO ground state and the possible BCS superfluid excited state (by enforcing $Q = 0$) to check the stability of the FFLO state against the finite temperature effect.

Phase diagram and mechanism for FFLO phase: In Fig. 1, we plot the phase diagrams of the Fermi gas with respect to h, $1/K_F a_s$, and αK_F. Without SO coupling (Fig. 1a), our result agrees well with that in pre-

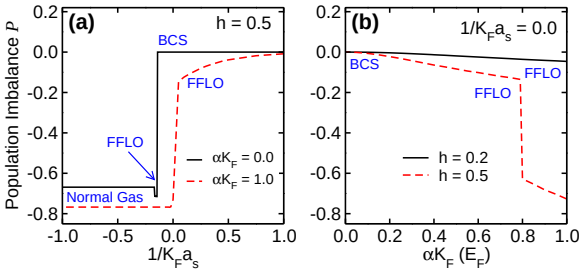

FIG. 3: (Color online). Population imbalance $P = \delta n/n$ as a function of the scattering interaction (a) and the SO coupling strength (b).

vious literatures using the mean-field approximation [18] or quantum Monte Carlo [52]. We see the FFLO phase exists only within an extremely small regime in the phase diagram. Furthermore, the energy difference per particle between the FFLO state and the possible BCS superfluid state is extremely small (see Fig. 4d), therefore the Fermi gas may not relax to the FFLO state considering the realistic temperature in experiments [13], even if the FFLO state is the true ground state. With increasing SO strength, the parameter region of the FFLO phase is greatly enlarged. In Fig. 1d, we see that the critical Zeeman field for the transition between the BCS superfluid and FFLO phase is greatly reduced, but always larger than zero because of the required time-reversal symmetry breaking for the FFLO phase.

The enlarged parameter region for the FFLO state in Fig. 1 can be understood from the deformation of the Fermi surface due to the SO coupling and the in-plane Zeeman field. Without the SO coupling, the Zeeman field (no matter which direction) yields two concentric spheres (Fig. 2a) of the Fermi surface, and only singlet pairing between different pseudospins (i.e., two eigenstates of H_0) is allowed due to the SU(2) symmetry of the Hamiltonian. With increasing Zeeman fields, the Fermi surface mismatch increases the energy cost of the BCS superfluid. In a strong Zeeman field the superfluid has to break the spatial symmetry to lower the accumulated energy, therefore the FFLO state emerges, but only survives in a small parameter region due to the Pauli depairing effect. Such depairing effect in strong Zeeman fields can be circumvented using the SO coupling, which allows both singlet and triplet pairings [41, 53, 54] (the later is insensitive to the depairing effect) because the pseudospin state is a spin mixed state with strong momentum dependence [40]. In the presence of SO coupling and an in-plane Zeeman field, the Fermi surfaces become anisotropic and the center of the Fermi surface is also shifted accordingly (Fig. 2b). Therefore the regular BCS superfluid, which is preferred for a symmetric Fermi surface, is greatly suppressed, and the FFLO state becomes energetically favorable in a much wider parameter region, as observed in Fig. 1. Note that without SO coupling (Fig. 2a), the system has the rotation symmetry, therefore Q can be along any direction. The SO coupling breaks the rotation symmetry, and forces Q to along the direction of the asymmetric axis (thus Q is unique).

The FFLO phase is induced by the interplay between asymmetry of Fermi surface and superfluid order, instead of the interplay between magnetism and superconducting order in solid materials. In our model the only spin polarization is along the σ_x axis (i.e., $\langle\sigma_z\rangle = 0$, $\langle\sigma_y\rangle = 0$), thus we define the the population imbalance as $P = \delta n/n$ with $\delta n = \langle\sigma_x\rangle$. In Fig. 3, we plot P with respect to $1/K_F a_s$ and αK_F. Without SO coupling, the BCS superfluid breaks down at $P \sim 0.669$, in consistent with previous results [13, 18]. When the SO coupling is applied, the FFLO phase can emerge with a much smaller population imbalance ($P \sim 0.1$ - 0.2). From Fig. 3, we see that the SO coupling generally enhances the population imbalance in the normal phase, however the emergence of the FFLO does not ocuur in this large population imbalance region. Therefore the FFLO phase cannot originate from the interplay between magnetism and superconducting order which is the major driving force for tranditional FFLO superfluid in the spin-polarized Fermi gas (withoug SO coupling) and 2D solid state materials.

Stability and measurement of of FFLO phase: To characterize the FFLO state, in Figs. 4, we plot the chemical potential μ and the order parameter Δ in the BCS-BEC crossover. For comparison, we also plot μ and Δ for the possible BCS superfluid state (by enforcing $Q = 0$). In the weak BCS limit Δ is exponentially small, therefore a small population imbalance can destroy the superfluid [14]. In the BEC side, the fermions form tightly bound molecules and the influence of Zeeman field and SO coupling is negligible. Therefore the only relevant parameter regime for the observation of FFLO states should be near the unitary regime. In the FFLO regime, Δ for the FFLO state is smaller than that for the assumed BCS superfluid to reduce the FFLO energy. In Fig. 4c, we plot Q versus the scattering interaction, which also confirms that the SO coupling can greatly increase the parameter region for the FFLO phase.

An experimentally observable FFLO state requires a large energy difference between the FFLO ground state and the possible BCS superfluid excited state so that the FFLO state can survive at finite temperature. In Fig. 4d, we plot the free energy difference per particle between FFLO state and the BCS superfluid, $\delta F = (F_{\rm FFLO} - F_{\rm BCS})/nE_F$, with $F = \Omega + \mu n$. The stability of the FFLO state has not been emphasized in previous literatures [19, 22–24, 26–28]. For FFLO states without SO coupling we find $\delta F \sim 10^{-4} E_F$, which is much smaller than the experimental coldest temperature ($T \sim 0.05 E_F$) [13, 55]. Therefore the FFLO state cannot be observed even the exact parameter region has been reached. While in our model the energy difference per particle is greatly enhanced to $\sim 0.04 E_F$, which makes the FFLO state ac-

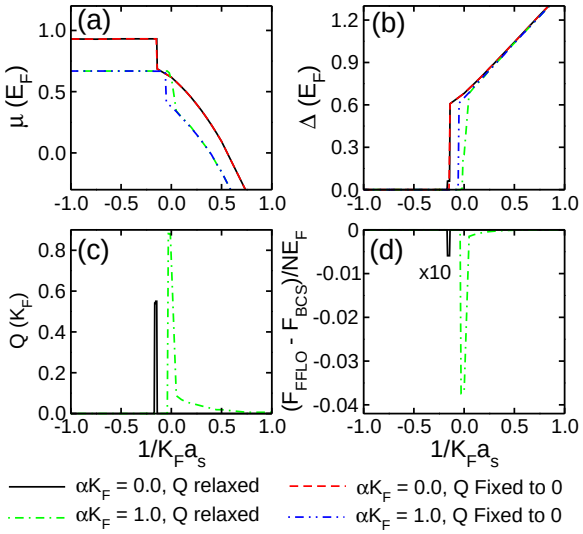

FIG. 4: (Color online). BEC-BCS crossover in the presence of SO coupling and an in-plane Zeeman field. $h = 0.5E_F$ and $\alpha K_F = 0.0$ and $1.0E_F$. In (a) and (b), the solid line and dashed dotted line are obtained by minimizing the total free energy with respect to Δ, μ and $\mathbf{Q}$, while the dashed line and dashed double dotted line are obtained by enforcing $Q = 0$ (thus no FFLO states). (c) Plot of Q as a function of the scattering interaction. (d) The free energy ($F = \Omega + \mu n$) difference between the FFLO state and the possible BCS superfluid.

cessible with realistic experimental temperature. Such a large energy difference is another major advantage of our scheme over previous Zeeman field [18–23] or optical lattice [24, 26–28] schemes.

So far we only consider the FFLO state using a simplified pairing $\Delta(\mathbf{r}) = \Delta e^{i\mathbf{Q}\cdot\mathbf{r}}$, while the true pairing of the FFLO state may be complicated. Because the FFLO state depends strongly on the nesting of the Fermi surface, the order parameter may be composed of multiple vectors [6, 56], *i.e.*, $\Delta(\mathbf{r}) = \Delta(\mathbf{Q}_1, \mathbf{Q}_2, \cdots)$ (e.g., the LO state with $\mathbf{Q}$ and $-\mathbf{Q}$), whose stability depends strongly on the detailed structure of the Fermi surface and thus cannot been fully ruled out [56]. However, the major findings of our work are intact even for very complex pairings because different choices of the order parameter are mainly used to further reduce the total energy of the FFLO state, thus further enhance our major findings.

The FFLO wavevector $\mathbf{Q}$ may be measured directly using the time-of-flight images [24, 57], where momentum distribution shows a peak at $\mathbf{r} = \hbar\mathbf{Q}t/m$. Because $\mathbf{Q}$ is unique in our system, repeated measurements can be used to determine $\mathbf{Q}$ precisely. The superfluidity of the FFLO states can be demonstrated through the rotation of the system, where the generated vortices provides unambiguous signature of superfluidity [58]. Near the boundary of different phases the vortices may be unstable due to strong damping effects [13], however in the middle of the FFLO phase (only possible with a large parameter region for the FFLO state), we expect the damping effect to be small, similar as that in the BCS superfluid state.

Comparision to solid state systems: We emphasize that our system has no direct solid state analogy although we note that FFLO states were also studied recently in 2D spin-orbit coupled superconductors with in-plane magnetic fields [59–61]. Our scheme is different from these 2D superconductors in the following aspects:

(I) Different driving mechanism: in 2D superconductors, FFLO phases are mainly induced by strong magnetic field and the role of SO coupling is to enhance the second critical magnetic field H_{c2} between superconducting and normal states [59, 60]. While in our 3D Fermi gases, FFLO phases are induced by the asymmetric Fermi surface, and are present even with a weak Zeeman field (see Fig. 1d) and a small population imbalance (see Fig. 3). (II) 3D vs 2D: It is well known that in 2D and at finite temperature the mean field theory does not work and there is no long range superconducting order (including FFLO) due to phase fluctuations [34–36]. In contrast, the mean-field theory works well, at least qualitatively, in 3D degenerate Fermi gases, which can support long-range FFLO order at finite temperature. (III) BCS-BEC crossover vs weak BCS limit: Our study focuses on the BCS-BEC crossover (strong coupling) physics (see Figs. 1, 3, and 4), in contrast with the weak BCS limit in 2D superconductors[59–61]; In our model the strong coupling regime can be achieved via Feshbach resonance[62]. (IV) Different experimental concerns: cold atomic gases are disorder free and FFLO phases can be observed directly in time-of-flight images; while in 2D superconductors disorder effects are important [60] and FFLO states can only be observed indirectly.

In summary, we show that the combination of SO coupling and in-plane Zeeman field can lead to a large and stable parameter region for the experimentally long-sought FFLO state even for 3D degenerate Fermi gases. Considering the recent experimental progress on the generation of the SO coupling in Bose and Fermi gases, our work provides a new exciting research direction for the study of SO coupled Fermi gases as well as the FFLO physics, which is essential for the understanding of important phenomena in many branches of physics, ranging from solid state superconductors to astrophysics.

Acknowledgement: Z.Z, X.Z, and G.G are supported by the National 973 Fundamental Research Program (Grant No. 2011cba00200), the National Natural Science Foundation of China (Grant No. 11074244). M.G and C.Z are supported by ARO (W911NF-12-1-0334), DARPA-YFA (N66001-10-1-4025), AFOSR (FA9550-11-1-0313), and NSF-PHY (1104546).

* Email: skylark.gong@gmail.com

† Email: xbz@ustc.edu.cn
‡ Email: chuanwei.zhang@utdallas.edu

[1] P. Fulde, and R. A. Ferrell, Phys. Rev. **135**, A550 (1964).
[2] A. I. Larkin, and Yu. N. Ovchinnikov, Zh. Eksp. Teor. Fiz. **47**, 1136 (1964).
[3] A. I. Larkin, and Yu. N. Ovchinnikov, Sov. Phys. JETP **20**, 762 (1965).
[4] A. Buzdin, Y. Matsuda, and T. Shibauchi, Europhys. Lett., **80**, 67004 (2007).
[5] M. D. Croitoru, M. Houzet and A. I. Buzdin, Phys. Rev. Lett. **108**, 207005 (2012).
[6] Y. Matsuda, and H. Shimahara, J. Phys. Soc. Jpn. **76**, 051005 (2007).
[7] K. Gloos, R. Modler, H. Schimanski, C. D. Bredl, C. Geibel, F. Steglich, A. I. Buzdin, N. Sato, and T. Komatsubara, Phys. Rev. Lett. **70**, 501 (1993).
[8] A. Bianchi, R. Movshovich, C. Capan, P. G. Pagliuso, and J. L. Sarrao, Phys. Rev. Lett. **91**, 187004 (2003).
[9] J. Singleton, J. A. Symington, M-S Nam, A. Ardavan, M. Kurmoo, and P. Day, J. Phys.: Condens. Matter **12**, L641 (2000).
[10] R. Lortz, Y. Wang, A. Demuer, P. H. M. Böttger, B. Bergk, G. Zwicknagl, Y. Nakazawa, and J. Wosnitza, Phys. Rev. Lett. **99**, 187002 (2007).
[11] R. Casalbuoni and G. Narduli, Rev. Mod. Phys. **76**, 263 (2004).
[12] M. G. Alford, K. Rajagopal, T. Schaefer, A. Schmitt, Rev. Mod. Phys. **80**, 1455 (2008).
[13] M. W. Zwierlein, A. Schirotzek, C. H. Schunck, and W. Ketterle, Science **311**, 492 (2006).
[14] M. W. Zwierlein, C. H. Schunck, A. Schirotzek, and W. Ketterle, Nature **442**, 54 (2006).
[15] G. B. Partridge, W. Li, R. I. Kamar, Y.-A. Liao and R. G. Hulet, Science, **311**, 503 (2006).
[16] G. B. Partridge, W. Li, Y. A. Liao, R. G. Hulet, M. Haque, and H. T. C. Stoof, Phys. Rev. Lett. **97**, 190407 (2006).
[17] Y.-I. Shin, C. H. Schunck, A. Schirotzek, and W. Ketterle, Nature **451**, 689 (2008).
[18] H. Hu and X.-J. Liu, Phys. Rev. A **73**, 051603(R), (2006).
[19] L. He, M. Jin and P. Zhuang, Phys. Rev. B **74**, 024516 (2006).
[20] M. M. Parish, F. M. Marchetti, A. Lamacraft, and B. D. Simons, Nature Physics **3**, 124 (2007).
[21] M. Iskin, C. A. R. Sa de Melo, Phys. Rev. Lett. **97**, 100404 (2006).
[22] D. E. Sheehy and L. Radzihovsky, Ann. Phys. **322**, 1790 (2007).
[23] Aurel Bulgac and Michael McNeil Forbes, Phys, Rev. Lett. **101**, 215301 (2008).
[24] T. K. Koponen, T. Paananen, J-P Martikainen, and P. Törma, Phys. Rev. Lett. **99**, 120403 (2007).
[25] E. Zhao, and W. V. Liu, Phys. Rev. A **78**, 063605 (2008).
[26] Y. Okawauchi and A. Koga, arxiv:1204.4187v1.
[27] Jeroen P. A. Devreese, Sergei N. Klimin, and Jacques Tempere, Phys. Rev. A **83**, 013606 (2011).
[28] Jeroen P. A. Devreese, Michiel Wouters, and Jacques Tempere, Phys. Rev. A **84**, 043623 (2011).
[29] Y.-A. Liao, A. S. C. Rittner, T. Paprotta, W. Li, G. B. Partridge, R. G. Hulet, S. K. Baur, and E. J. Mueller, Nature, **467**, 567 (2010).
[30] G. Orso, Phys. Rev. Lett. **98**, 070402 (2007).
[31] H. Hu, X.-J. Liu, and P. D. Drummond, Phys. Rev. Lett. **98**, 070403 (2007).
[32] M. M. Parish, S. K. Baur, E. J. Mueller, and D. A. Huse, Phys. Rev. Lett. **99**, 250403 (2007).
[33] H. Lu, L. O. Baksmaty, C. J. Bolech, H. Pu, Phys. Rev. Lett. **108**, 225302 (2012).
[34] P. C. Hohenberg, Phys. Rev. **158**, 383 (1967).
[35] V. L. Berezinskii, Sov. Phys. JETP **32**, 493 (1971).
[36] J. M. Kosterlitz and D. Thouless, J. Phys. C **5**, L124 (1972); **6**, 1181 (1973).
[37] Y.-J. Lin, K. Jimenez-Garcia, and I. B. Spielman, Nature **471**, 83 (2011).
[38] P. Wang, Z.-Q. Yu, Z. Fu, J. Miao, L. Huang, S. Chai, H. Zhai, J. Zhang, Phys. Rev. Lett. **109**, 095301 (2012).
[39] L. W. Cheuk, A. T. Sommer, Z. Hadzibabic, T. Yefsah, W. S. Bakr, M. W. Zwierlein, Phys. Rev. Lett. **109**, 095302 (2012).
[40] C. Zhang, S. Tewari, R. M. Lutchyn, and S. Das Sarma, Phys. Rev. Lett. **101**, 160401 (2008).
[41] M. Gong, S. Tewari and C. Zhang, Phys. Rev. Lett. **107**, 195303 (2011).
[42] J. Zhou, W. Zhang and W. Yi, Phys. Rev. A **84**, 063603 (2011).
[43] M. Iskin and A. L. Subasi, Phys. Rev. Lett. **107**, 050402 (2011).
[44] M. Gong, G. Chen, S. Jia, and C. Zhang, Phys. Rev. Lett. **109**, 105302 (2012).
[45] X.-J. Liu, L. Jiang, H. Pu, and H. Hu, Phys. Rev. A **85**, 021603(R) (2012).
[46] M. Iskin, Phys. Rev. A. **85**, 013622 (2012).
[47] T. D. Stanescu, C. Zhang, and V. Galitski, Phys. Rev. Lett. **99**, 110403 (2007).
[48] J. Dalibard, F. Gerbier, G. Juzeliūnas, and P. Öhberg, Rev. Mod. Phys. **83**, 1523 (2011).
[49] Y. Zhang, L. Mao, and C. Zhang, Phys. Rev. Lett. **108**, 035302 (2012).
[50] C. Zhang, Phys. Rev. A **82**, 021607(R) (2010).
[51] Without SO coupling, the Zeeman field can be applied through adjusting the population imbalance between two spin states. While in the presence of SO coupling, the number of atoms at each spin channel is not conserved anymore, and the population imbalance can be tuned only through the external Raman lasers (Zeeman field).
[52] J. Carlson and S. Reddy, Phys. Rev. Lett. **95**, 060401 (2005).
[53] H. Hu, L. Jiang, X.-J. Liu, and H. Pu, Phys. Rev. Lett. **107**, 195304 (2011).
[54] Z.-Q. Yu, and H. Zhai, Phys. Rev. Lett. **107**, 195305 (2011).
[55] M. Greiner, C. A. Regal, and D. S. Jin, Phys. Rev. Lett. **94**, 070403 (2005).
[56] L. Bulaevskii, A. Buzdin, and M. Maley, Phys. Rev. Lett. **90**, 067003 (2003).
[57] J. Steinhauer, N. Katz, R. Ozeri, N. Davidson, C. Tozzo, F. Dalfovo, Phys. Rev. Lett. **90**, 060404 (2003).
[58] M.W. Zwierlein, J. R. Abo-Shaeer, A. Schirotzek, C.H. Schunck, and W. Ketterle, Nature **435**, 1047 (2005).
[59] Victor Barzykin and Lev P. Gor'kov, Phys. Rev. Lett. **89**, 227002 (2002).
[60] K. Michaeli, A. C. Potter, and P. A. Lee, Phys. Rev. Lett. **108**, 117003 (2012).
[61] H. Tanaka, H. Kaneyasu, and Y. Hasegawa, J. Phys. Soc. Japan **76**, 024715 (2007).
[62] Cheng Chin, Rudolf Grimm, Paul Julienne, and Eite Tiesinga, Rev. Mod. Phys. **82**, 1225 (2010).